Microchimica Acta (2018) 185: 284
https://doi.org/10.1007/s00604-018-2817-3

ORIGINAL PAPER

Water-soluble polymer dots formed from polyethylenimine and glutathione as a fluorescent probe for mercury(II)

Dan Luo[1] · Shi Gang Liu[1] · Nian Bing Li[1] · Hong Qun Luo[1]

Received: 9 April 2018 / Accepted: 24 April 2018 / Published online: 8 May 2018

Abstract

Water-soluble fluorescent polymer dots (PDs) were prepared from polyethylenimine and glutathione and are shown to be viable fluorescent probes for selective and sensitive determination of Hg(II). The PDs possess bright blue fluorescence (with excitation/emission peaks at 340/462 nm) which is quenched on addition of Hg(II). Based on these findings, a fluorometric assay was worked out. Fluorescence linearly drops in the 0.1 to 100 μM Hg(II) concentration range, and the limit of detection is 32 nM.

Keywords Hg^{2+} analysis · Environmental samples · Industrial waste water · Heavy metal ions · Electron transfer · Stern-Volmer plot · Non-conjugated polymers · Dynamic quenching

Introduction

Polymers with strong fluorescence emission are generally constructed by conjugated polymers which own conjugated main chain or π-aromatic building blocks [1, 2]. However, researchers have discovered that some non-conjugated polymers can emit strong fluorescence under suitable conditions, such as poly(amidoamine), polyurethane, polyethylenimine, poly(ether amide), and so on [3, 4]. The discovery is of great significance, because these polymers lack conjugated polymer structures and do not contain any typical chromophore. Thus, the fluorescence emission is unexpected. It is believed that the fluorescence-emitting moieties may be some heteroatom-containing double bonds (C=O, C=N, C=S, etc.), although the bonds cannot emit fluorescence under normal conditions [5]. But some argue that the macromolecules can form nanostructures under suitable conditions, which cause the fluorescence emission [6]. Overall, the fluorescence mechanism of these non-conjugated polymers is still under investigation. Nevertheless, due to their special structures and affluent terminal groups, these non-conjugated fluorescent polymers have well hydrophilic property, flexible chains, and adjustable structures. Therefore, they have great potential in the field of chemistry, material, and biology as a new type of fluorescent material.

As one of the most hazardous metal contaminants, Hg^{2+} has deleterious influence on the environment and human health even at a low concentration. Once Hg^{2+} is introduced into the real water environment, microorganisms can convert the inorganic mercury into methyl mercury, which is easily accumulated in organisms through the food chain over time [7, 8]. Methyl mercury has neurotoxic effect and is harmful to the central nervous of human and other living organisms [9–11]. Therefore, it is of considerable importance to develop Hg^{2+} determination methods with good sensitivity, specificity, and rapidity [12]. Conventional techniques for Hg^{2+} detection include high performance liquid chromatography, surface-enhanced Raman spectroscopy, electrochemical methods, inductively coupled plasma-mass spectrometry, and so on [11–15]. Among these techniques, fluorescent probes have advantages in low expense, broad linearity, and high sensitivity. Furthermore, the instrumentation is simple to operate and the response time is fast [16–20].

In this work, we report a fluorescent probe of Hg^{2+} on the basis of a kind of novel and water-soluble non-conjugated

Electronic supplementary material The online version of this article (https://doi.org/10.1007/s00604-018-2817-3) contains supplementary material, which is available to authorized users.

✉ Nian Bing Li
linb@swu.edu.cn

✉ Hong Qun Luo
luohq@swu.edu.cn

[1] Key Laboratory of Eco-environments in Three Gorges Reservoir Region (Ministry of Education), School of Chemistry and Chemical Engineering, Southwest University, Chongqing 400715, People's Republic of China

polymer dots. The polymer dots were prepared by polyethyleimine (PEI) and glutathione (GSH), denoted as G-PEI PDs. Hg^{2+} was able to sensitively and selectively quench the fluorescence of the PDs. Therefore, the PDs were used to create a novel fluorescent probe for detecting Hg^{2+} in environmental water. Scheme 1 illustrates the principle, including preparation of the G-PEI PDs and detection of Hg^{2+} by using the PDs as a probe. Compared to other approaches, our method is novel, favorable, and meaningful. First, the GSH contains sulfur atoms and can combine with Hg^{2+} forcefully. The PEI has good water solubility, making applications of the PDs in aqueous solution possible. Therefore, selective detection of Hg^{2+} was achieved in water phase. Second, the synthetic process does not need exacting terms, just one-step, and the materials are environmentally friendly without the need of organic solvents. Third, this work using the non-conjugated fluorescent polymer dots to fabricate a mercury ion probe might be helpful to accelerate the application development of new polymer dots in environmental, medical, and other fields.

Experimental section

Materials

Polyethylenimine (PEI, $M_w = 10{,}000$, 99%) and glutathione (GSH) were purchased from Aladdin Ltd., Shanghai, China (http://www.aladdin-e.com). Britton-Robinson (BR) buffers (0.04 M, pH 3.0–11.0) were made by mixing 0.2 M NaOH and a mixture of 0.04 M CH_3COOH, H_3PO_4, and H_3BO_3 according to standard protocols. Ultrapure water (18.2 MΩ cm) was used through this study, and all chemicals were of analytical reagent grade and were used without further purification.

Apparatus

A Hitachi F-2700 fluorescence spectrophotometer (Hitachi, Japan, http://www.hitachi.com) was used to record fluorescence spectra. The slit widths of both excitation and emission were set as 10.0 nm; the scan wavelength speed was fixed as 1500 nm min^{-1}; the voltage of photomultiplier tube (PMT) was 400 V. A UV-vis 2450 spectrophotometer (Shimadzu, Japan, https://www.shimadzu.com) was used to record UV-vis absorption spectra. pH values of the solutions were detected by a Mettler Toledo FE28 pH meter (Mettler-Toledo, Switzerland, https://www.mt.com/us/en/home.html). Transmission electron microscopy (TEM) measurement was taken on a JEM 1200EX transmission electron microscope (JEOL, Japan, https://www.jeol.co.jp/en). A Bruker IFS 113v spectrometer (Bruker, Germany, https://www.bruker.com) was used to perform the Fourier transform infrared (FT-IR) spectrum test. Fluorescence lifetime decays were conducted on an Edinburgh FL 920 fluorescence spectrometer (Edinburgh, U.K., www.edinst.com).

Preparation of G-PEI polymer dots

The G-PEI PDs were prepared by mixing 1 mL of GSH aqueous solution (0.1 M) and 1 mL of PEI aqueous solution (0.1 g mL^{-1}), and this mixture was diluted to 10 mL by ultrapure water. Afterwards, the mixture was stirred for about 3 min by magnetic stirrer, and heated at 200 °C for 4 h. After that, the reaction system was cooled down to the ambient temperature spontaneously. At last, to purify the PDs and eliminate the interference from small molecules, dialyzing the PD solution against ultrapure water through a dialysis membrane (molecular weight cutoff of 500 Da) for 24 h was implemented. The pale yellow product inside the dialysis bag was the PD solution and was collected for next study.

Quantum yield measurements of G-PEI polymer dots

The quantum yield of the G-PEI PDs was calculated by the following equation:

$$\varphi_x = \varphi_{st}\,(K_x/K_{st})(\eta_x/\eta_{st})^2 \quad (1)$$

where φ is the quantum yield, K is the slope, η is the refractive index. The subscript x refers to the samples to be tested, in this work it is the G-PEI PDs. The subscript st refers to the

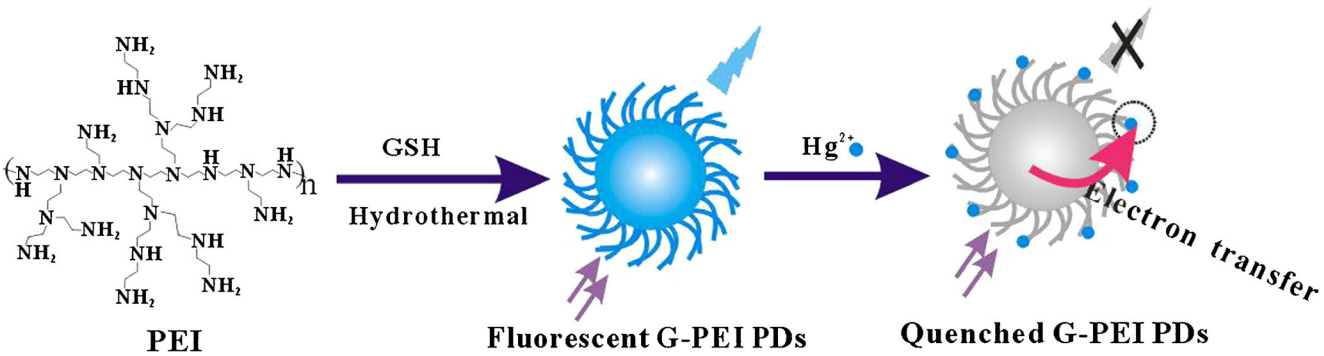

Scheme 1 Schematic illustration of the synthesis of G-PEI PDs and the Hg^{2+} determination based on the G-PEI PDs

standard samples of known quantum yield, for instance, quinine sulfate (QS) is applied in this research. The quinine sulfate (literature $\varphi = 0.54$) was dispersed in 0.1 M H_2SO_4 ($\eta = 1.33$) and the PDs was dispersed in a BR buffer ($\eta = 1.33$).

Fluorescence determination of Hg^{2+}

The detecting procedures for fluorescence determination of Hg^{2+} were as follows. G-PEI PD solution (20 μL, 7.4 mg mL^{-1}) was added to 930 μL of BR buffer (0.04 M, pH 5.0), and then 50 μL of Hg^{2+} with different concentrations was mixed with the mixture. The mixture was then stirred for about 5 s and reacted for about 2 min. Overall processes were implemented at ambient temperature. Then, the fluorescence spectra were obtained by exciting all samples at the maximum excitation wavelength of 340 nm. The fluorescence intensities were recorded at the maximum emission wavelength of 462 nm. The fluorescence intensities of the PDs with and without the addition of Hg^{2+} were regarded as F and F_0, respectively.

Application in environmental water samples

Jialing River water samples were got from the Jialing River (Chongqing, China), tap water samples were straight obtained from our laboratory, and chemical plant waste water samples were obtained from a local chemical plant. In order to remove the suspended impurities, total raw water samples were centrifuged at 12000 rpm for 15 min to get the supernatant before detection. To inspect the accuracy of the system, various concentrations of Hg^{2+} (1.0, 10, and 20 μM) were added to the environmental water samples. For fluorescence detection, 20 μL of 7.4 mg mL^{-1} G-PEI PD solution and 10 μL of the water samples were added to 970 μL of BR buffer (0.04 M, pH 5.0) containing ethylenediaminetetraacetate (EDTA) with an ultimate concentration of 100 μM. Other procedures were the same as described above.

Results and discussion

Characterization of G-PEI polymer dots

The G-PEI PDs were characterized by fluorescence, TEM, and FT-IR spectroscopy. The fluorescence spectral characterizations of PDs were recorded. As shown in Fig. 1a, the maximum emission wavelength is at 462 nm when excited at 340 nm. The photographs (inset of Fig. 1a) indicate that the PD solution is pale yellow under natural light, which is different from colorless PEI and GSH aqueous solution, while under UV light (365 nm) the PD solution exhibits bright blue fluorescence. The fluorescence emission spectra of the PDs at different excitation wavelengths are shown in Fig. 1b. No obvious shift is observed when the excitation wavelength is varied over the range from 300 to 380 nm. In addition, the quantum yield (excited at 340 nm) of the PDs in a pH 5.0 BR buffer was measured to be 0.027 (Fig. S1). As shown in Fig. 1c, the TEM image indicates that the PDs are almost monodisperse. The inset of Fig. 1c illustrates that the diameter range of the PDs is 2.15–8.35 nm with an average size about 5.41 nm, indicating that the PDs can be dispersed well in water. However, high resolution TEM image of the PDs was not obtained because the polymer dots would be disrupted under high-power electron beam, which demonstrated that the PDs were not carbonized materials. FT-IR spectroscopy was used to further recognize the functional groups that existed in the PDs. As shown in Fig. 1d, the polymer dots have several characteristic absorption bands of GSH, meaning the binding of GSH to the surface of the PDs. The absorption centered at 1575 and 1465 cm^{-1} are corresponding to the stretching vibration of carboxyl group bonds; the absorption centered at 3411 cm^{-1} is the overlap of the absorption of -OH bonds and N-H bonds; the absorption bands located at 688 and 617 cm^{-1} are corresponding to the stretching vibration of C-S bonds. In addition, a sharp peak assigned to the vibration absorption of amide linkages (-CONH-) is found at 1633 cm^{-1} on the FT-IR spectrum which indicates that the carboxy groups of GSH have reacted with the amine groups of PEI by dehydration acylation reaction to form the amide linkages.

Hg^{2+}-induced fluorescence quenching of G-PEI polymer dots

As shown in Fig. 2a, the presence of Hg^{2+} decreases the fluorescence intensity of the PDs notably, but there is no obvious effect on the maximum emission wavelength. With and without the addition of Hg^{2+}, the UV-vis absorption spectra of GSH, PEI, and G-PEI PDs were recorded and are shown in Fig. 2b. The PDs exhibit a new wide absorption band over the range from 300 to 400 nm with an absorption peak located at 325 nm, while sole PEI and GSH have no significant absorption above 300 nm. The new absorption band can be ascribed to the $n \rightarrow \pi^*$ transitions [21–23]. With the introduction of Hg^{2+}, the absorption peak at 325 nm of the PDs has no remarkable shift. This result suggests that the probable quenching mechanism is dynamic quenching, which is related to the excited states but not to the ground states.

Optimization of experimental parameters

The following parameters were optimized: (a) Sample pH value; (b) reaction time; (c) ionic strength. Respective data and figures are given in Fig. S2. The following experimental conditions were found to give the best results: (a) best sample pH

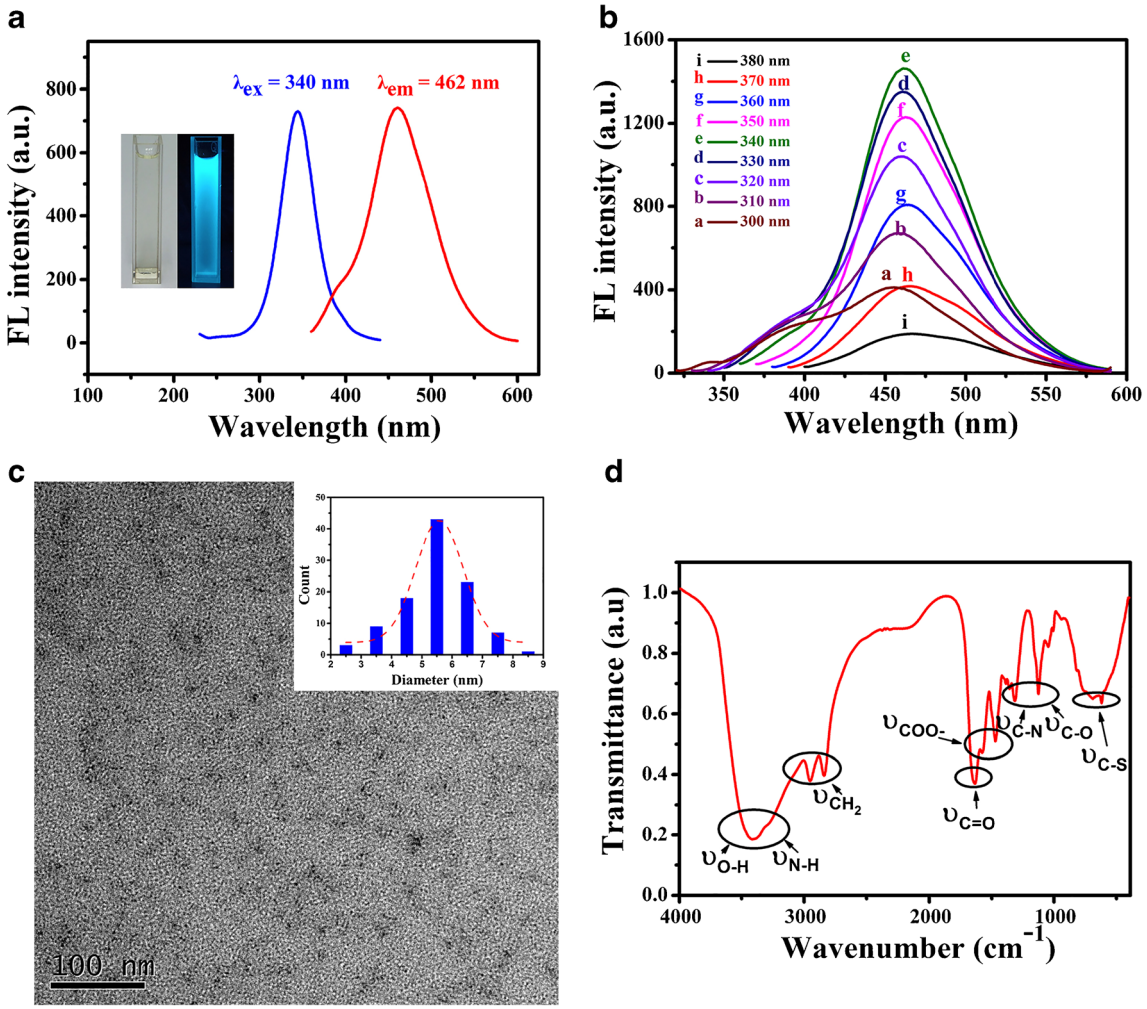

Fig. 1 **a** Fluorescence emission and excitation spectra of the G-PEI PDs (0.148 mg mL^{-1}) in aqueous solution (λ_{ex} = 340 nm, λ_{em} = 462 nm). Inset shows the photographs of the G-PEI PDs under the irradiation of UV light (right) and natural light (left). **b** Fluorescence emission spectra of the G-PEI PDs (0.74 mg mL^{-1}) under different excitations. **c** TEM image of the G-PEI PDs. Inset shows the size distribution of the G-PEI PDs. **d** FT-IR spectrum of the G-PEI PDs

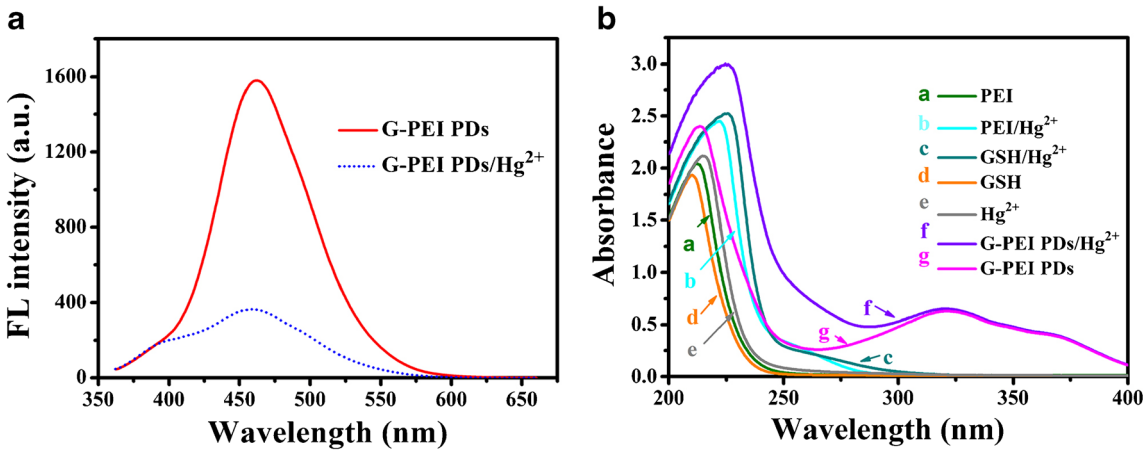

Fig. 2 **a** Fluorescence spectra of the G-PEI PDs with and without the addition of Hg^{2+}. Conditions: G-PEI PDs, 0.74 mg mL^{-1}; Hg^{2+}, 30 μM; BR buffer, pH 5.0. **b** UV-vis absorption spectra of (*a*) PEI, (*b*) PEI + Hg^{2+}, (*c*) GSH + Hg^{2+}, (*d*) GSH, (*e*) Hg^{2+}, (*f*) G-PEI PDs + Hg^{2+} and (*g*) G-PEI PDs. Concentrations: GSH, 0.01 M; PEI, 0.01 g mL^{-1}; G-PEI PDs, 7.4 mg mL^{-1}; Hg^{2+}, 30 μM

value: 5.0; (b) optimal reaction time: 2 min; (c) ionic strength: little influence except for samples with high ionic strength (over 0.1 M).

Fluorescence determination of Hg^{2+}

Because of the estimable change in the fluorescence intensity of the G-PEI PDs in the presence of Hg^{2+}, Hg^{2+} with various concentrations were added to the PD solutions under the optimum experimental conditions to assess the sensitivity. As shown in Fig. 3a, increasing concentration of Hg^{2+} decreases the fluorescence intensity of the PDs gradually, and the Stern-Volmer plot is upward curved. By linear fitting, a linear equation $(F_0\text{-}F)/F$ = 0.0132 [Hg^{2+}] - 0.0276 is observed in the concentration range of 0.1–100 μM with a good linear relationship (R = 0.9915). A Stern-Volmer plot for the lower concentration range is shown in the inset of Fig. 3a. The limit of detection for Hg^{2+} is 32 nM on the basis of 3σ/slope (σ denotes the standard deviation of the background measure). Figure 3b shows the corresponding fluorescence spectra. As shown in Table S1, compared to other fluorescent probes for detecting Hg^{2+}, the PDs show more excellent performance with a wider linear range and a lower limit of detection, indicating that this method is novel, favorable, and meaningful to some extent.

Selectivity for Hg^{2+} determination

. To prove the selectivity of the PDs, seventeen metal ions including K^+, Na^+, Li^+, Ag^+, Co^{2+}, Sr^{2+}, Ba^{2+}, Pb^{2+}, Mg^{2+}, Cu^{2+}, Zn^{2+}, Fe^{2+}, Ni^{2+}, Cd^{2+}, Al^{3+}, Cr^{3+}, Fe^{3+}, fourteen anions containing F^-, Cl^-, Br^-, I^-, NO_2^-, NO_3^-, CH_3COO^-, S^{2-}, SiO_3^{2-}, CO_3^{2-}, SO_3^{2-}, SO_4^{2-}, PO_4^{3-}, $P_2O_7^{4-}$, and natural organic matter humic acid were used to evaluate their influence on the fluorescence intensity under the optimum conditions. All species concentrations were 50 μM, and all of the fluorescence detections were carried out under the same conditions. Most ions have no obvious influence on the fluorescence intensity, except that Co^{2+}, Cu^{2+}, and Fe^{3+} can also quench the fluorescence to some extent. Through further experiments, we found that the fluorescence quenched by Co^{2+}, Cu^{2+}, and Fe^{3+} can be recovered by adding EDTA with a final concentration of 100 μM, but EDTA had little influence on the fluorescence quenching by Hg^{2+}. Ultimately, adding EDTA to the real samples was chosen for detecting Hg^{2+} in environmental water to decrease the possible interference (Fig. 4). However, the influence of humic acid on fluorescence quenching is obvious (Fig. S3). Therefore, for effective detection of Hg^{2+} by the method, pretreatment such as digestion is required for a real sample containing humic acid. In addition, the need with UV excitation makes the probe prone to interference from biomatter, which may display background fluorescence under UV excitation. Besides, the UV light used for excitation may be screened off by UV absorbing molecules. Therefore, some pretreatments such as digestion and ultrafiltration are needed before the determination of Hg^{2+}. For example, we can carry out ultrafiltration when samples contain macromolecules. Overall, this method has some limitations. The pretreatments mentioned above would make experimentation inconvenient. In addition, the use of UV excitation can limit the applications of the probe in the field of biology.

Probable fluorescence quenching mechanism

Fluorescence quenching mechanisms include static quenching, dynamic quenching, Förster resonance energy transfer (FRET), photoinduced electron transfer (PET),

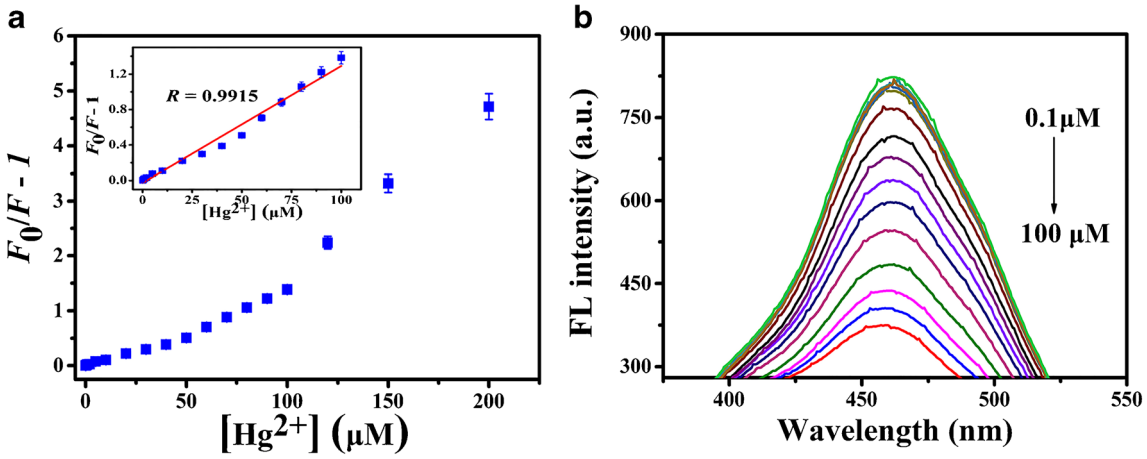

Fig. 3 **a** The fluorescence quenching efficiency (F_0/F - 1) is related to the concentration of Hg^{2+} over the range from 0 to 200 μM, and the inset shows the linear relationship between F_0/F - 1 and the concentration of Hg^{2+}. **b** Fluorescence spectra of G-PEI PDs with the addition of different concentrations of Hg^{2+} (from top to bottom: 0.1, 0.2, 0.5, 1, 2, 5, 10, 20, 30, 40, 50, 60, 70, 80, 90, 100 μM). Conditions: G-PEI PDs, 0.148 mg mL^{-1}; BR buffer, pH 5.0; excitation, 340 nm; emission, 462 nm

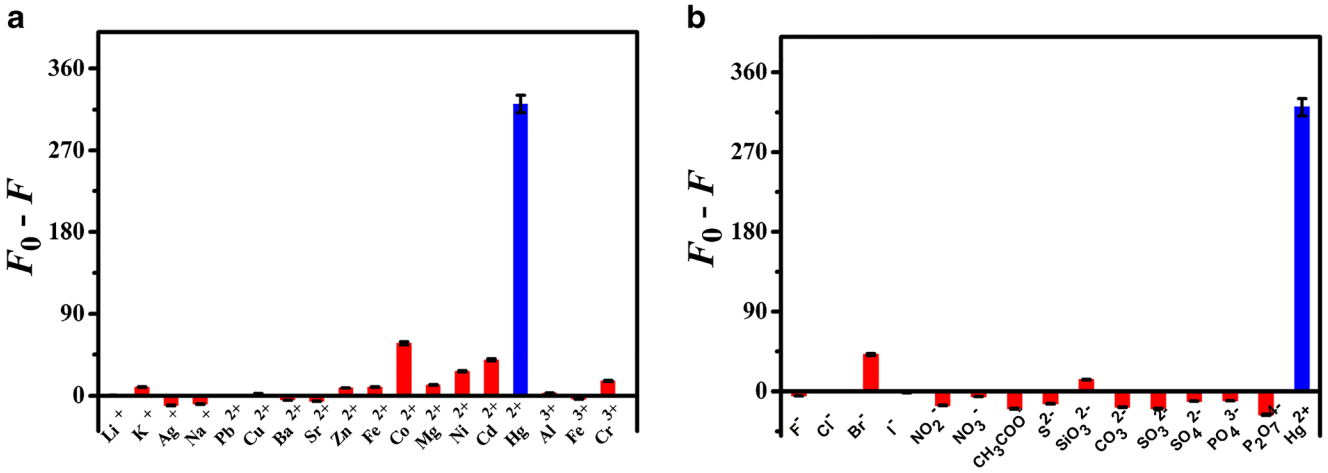

Fig. 4 Fluorescence quenching efficiency (F_0 - F) of various ions. Concentrations of all ions are 50 μM. Co^{2+}, Cu^{2+}, Fe^{3+}, and Hg^{2+} contain 100 μM EDTA, respectively. Conditions: G-PEI PDs, 0.148 mg mL^{-1}; BR buffer, pH 5.0; excitation, 340 nm; emission, 462 nm

surface energy transfer (SET), Dexter energy transfer (DET), and inner filter effect (IFE) [24, 25]. This work is only satisfied with some characteristics of dynamic quenching. For example, the lifetime of PDs would change in the absence and presence of quencher. As shown in Fig. 5a, the fluorescence decay in PDs/Hg^{2+} system is obtained as $\tau_D = 2.9$ ns and it is much less compared to that of the probe PDs ($\tau_D = 5.6$ ns), indicating that in the presence of Hg^{2+}, the fluorescence lifetime decreases. A rise of temperature can lead to the increase of the effect of dynamic quenching. It is because that the higher temperature means faster diffusion and more collisional quenching. As shown in Fig. 5b, the fluorescence intensity gradually decreases with increasing temperature, demonstrating that a dynamic quenching processes is operative.

In addition, on the basis of the previous research, the fluorescence quenching of polymer dots by analytes can be ascribable to the analytes binding on the surface of the polymer dots, which may trap the excited electron by electron transfer mechanism [26–28]. According to the images and data displayed above, the fluorescence quenching of the PDs by Hg^{2+} can be ascribed to the electron transfer process [29, 30]. On the one hand, dynamic fluorescence quenching can be interpreted that the excited states of polymer dots return to the ground states by the collision between the analytes and polymer dots with the mechanism of electron transfer [31]. On the other hand, plenty electron-rich groups and sulfur-bearing groups are on the surface of the PDs. Hence, when electron-deficient Hg^{2+}, which possesses empty *d* orbital and may be bound to the surface of the G-PEI PDs, is added to the PD solution, the fluorescence quenching appears via electron transfer. Overall, the quenching mechanism is ascribed to dynamic quenching induced by electron transfer in this work.

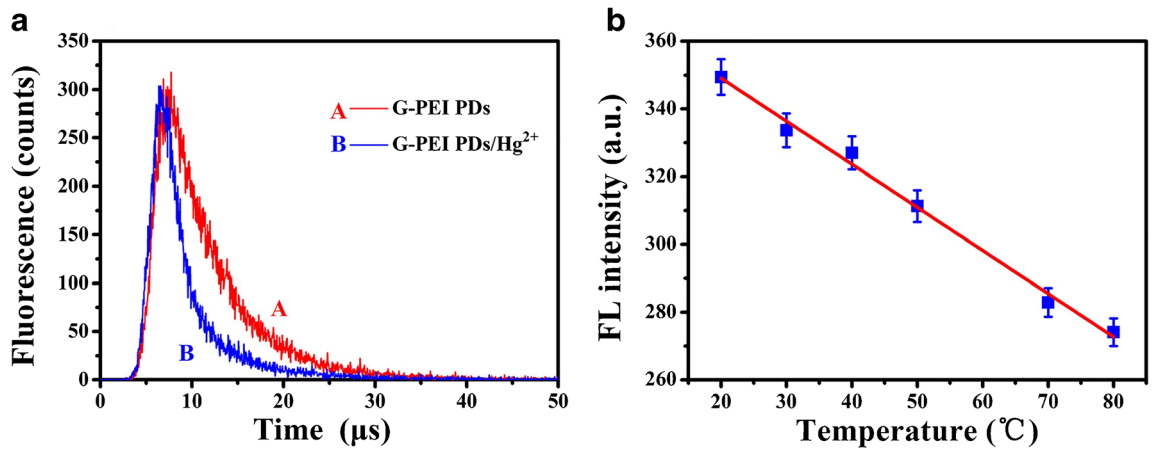

Fig. 5 **a** Time-resolved fluorescence spectra of G-PEI PDs with and without the addition of Hg^{2+}. **b** The influence that temperature made on the fluorescence intensity of the G-PEI PDs with the addition of Hg^{2+}. Conditions: G-PEI PDs, 0.148 mg mL^{-1}; Hg^{2+}, 30 μM; BR buffer, pH 5.0; excitation, 340 nm; emission, 462 nm

Application in environmental water samples

To explore the practical applicability for selective and sensitive determination of Hg^{2+} by this probe, we applied this method to detect Hg^{2+} in Jialing River water, tap water and chemical plant waste water samples. The varieties in the fluorescence intensities of PDs were tested in the presence of environmental water sample. Hg^{2+} with various concentrations and EDTA with an ultimate concentration of 100 μM were added to the mixture. No Hg^{2+} was found in Jialing River, tap water or chemical plant waste water samples. For the Hg^{2+}-added samples, the values measured by this method are in compliance with the added values for the concentration of Hg^{2+}. As listed in Table S2, the recoveries of Jialing River samples range from 90.3% to 104.2%, those of tap water samples range from 92.5% to 105.2%, and those of chemical plant waste water samples range from 91.0% to 107.0%. Also, low relative standard deviations (RSDs) (1.3–4.4%) can be found. The results explicitly illustrate that the method can be used to estimate the Hg^{2+} concentration in environmental water samples.

Conclusions

In summary, novel non-conjugated polymer dots, G-PEI PDs, with strong fluorescence were prepared by using GSH and PEI. On the basis of the fact that Hg^{2+} can quench the fluorescence of the PDs sensitively, a promising method with high sensitivity and selectivity for Hg^{2+} determination was developed. The application of the PD probe for Hg^{2+} detection has been tested in environmental water samples and satisfied results were gained, suggesting a potential method for environmental analysis. Furthermore, using the G-PEI PDs as a mercury ion probe can be helpful to accelerate the application development of new non-conjugated polymer dots in environmental, medical, as well as other fields. But this method also has a few limitations. For example, in complex real samples, pretreatments such as digestion, ultrafiltration, and addition of EDTA should be carried out to reduce the interference from other substances. These operations can make experimentation inconvenient. Overall, the defects cannot obscure the virtues. This method with a wider linear range and a lower detection limit indicates superior performance for Hg^{2+} detection in environmental water.

Acknowledgements Authors deeply acknowledge financial support for this work from the National Natural Science Foundation of China (No. 21675131), the Municipal Science Foundation of Chongqing City (CSTC-2015jcyjB50001), and the National Undergraduate Training Program for Innovation and Entrepreneurship (No.201610635036).

Compliance with ethical standards The author(s) declare that they have no competing interests.

References

1. Yao J, Yang M, Duan Y (2014) Chemistry, biology, and medicine of fluorescent nanomaterials and related systems: new insights into biosensing, bioimaging, genomics, diagnostics, and therapy. Chem Rev 114:6130–6178
2. Kim HN, Guo Z, Zhu W, Yoon J, Tian H (2011) Recent progress on polymer-based fluorescent and colorimetric chemosensors. Chem Soc Rev 40:79–93
3. Liu SG, Luo D, Li N, Zhang W, Lei JL, Li NB, Luo HQ (2016) Water-soluble nonconjugated polymer nanoparticles with strong fluorescence emission for selective and sensitive detection of nitro-explosive picric acid in aqueous medium. ACS Appl Mater Interfaces 8:21700–21709
4. Liu SG, Liu T, Li N, Geng S, Lei JL, Li NB, Luo HQ (2017) Polyethylenimine-derived fluorescent nonconjugated polymer dots with reversible dual-signal pH response and logic gate operation. J Phys Chem C 121:6874–6883
5. Lu H, Feng LL, Li SS, Zhang J, Lu HF, Feng SY (2015) Unexpected strong blue photoluminescence produced from the aggregation of unconventional chromophores in novel siloxane-poly(amidoamine) dendrimers. Macromolecules 48:476–482
6. Zhu SJ, Song YB, Shao JR, Zhao XH, Yang B (2015) Non-conjugated polymer dots with crosslink-enhanced emission in the absence of fluorophore units. Angew Chem Int Ed 54: 14626–14637
7. Boening DW (2000) Ecological effects, transport, and fate of mercury: a general review. Chemosphere 40:1335–1351
8. Harris HH, Pickering IJ, George GN (2003) The chemical form of mercury in fish. Science 301:1203–1203
9. Ariya PA, Amyot M, Dastoor A, Deeds D, Feinberg A, Kos G, Poulain A, Ryjkov A, Semeniuk K, Subir M, Toyota K (2015) Mercury physicochemical and biogeochemical transformation in the atmosphere and at atmospheric interfaces: a review and future directions. Chem Rev 115:3760–3802
10. Li WC, Tse HF (2015) Health risk and significance of mercury in the environment. Environ Sci Pollut Res 22:192–201
11. Zhang RZ, Chen W (2014) Nitrogen-doped carbon quantum dots: facile synthesis and application as a "turn-off" fluorescent probe for detection of Hg^{2+} ions. Biosens Bioelectron 55:83–90
12. Nolan EM, Lippard SJ (2008) Tools and tactics for the optical detection of mercuric ion. Chem Rev 108:3443–3480
13. Leermakers M, Baeyens W, Quevauviller P, Horvat M (2005) Mercury in environmental samples: speciation, artifacts and validation. Trac-Trends Anal Chem 24:383–393
14. Krishna MVB, Castro J, Brewer TM, Marcus RK (2007) Online mercury speciation through liquid chromatography with particle beam/electron ionization mass spectrometry detection. J Anal At Spectrom 22:283–291
15. Mor-Piperberg G, Tel-Vered R, Elbaz J, Willner I (2010) Nanoengineered electrically contacted enzymes on DNA scaffolds: functional assemblies for the selective analysis of Hg^{2+} ions. J Am Chem Soc 132:6878–6879
16. Zarlaida F, Adlim M (2017) Gold and silver nanoparticles and indicator dyes as active agents in colorimetric spot and strip tests for mercury(II) ions: a review. Microchim Acta 184:45–58
17. Xu H, Zhang K, Liu Q, Liu Y, Xie M (2017) Visual and fluorescent detection of mercury ions by using a dually emissive ratiometric nanohybrid containing carbon dots and CdTe quantum dots. Microchim Acta 184:1199–1206
18. Shamsipur M, Safavi A, Mohammadpour Z, Ahmadi R (2016) Highly selective aggregation assay for visual detection of mercury ion based on competitive binding of sulfur-doped carbon nanodots to gold nanoparticles and mercury ions. Microchim Acta 183: 2327–2335

19. Shi D, Yan F, Zhou X, Zheng T, Shi Y, Fu W, Chen L (2016) Preconcentration and fluorometric detection of mercury ions using magnetic core-shell chitosan microspheres modified with a rhodamine spirolactam. Microchim Acta 183:319–327
20. Tang W, Wang Y, Wang P, Di J, Yang J, Wu Y (2016) Synthesis of strongly fluorescent carbon quantum dots modified with polyamidoamine and a triethoxysilane as quenchable fluorescent probes for mercury(II). Microchim Acta 183:2571–2578
21. Li F, Liu C, Yang J, Wang Z, Liu W, Tian F (2014) Mg/N double doping strategy to fabricate extremely high luminescent carbon dots for bioimaging. RSC Adv 4:3201–3205
22. Amali AJ, Hoshino H, Wu C, Ando M, Xu Q (2014) From metal-organic framework to intrinsically fluorescent carbon nanodots. Chem Eur J 20:8279–8282
23. Sun X, Brueckner C, Lei Y (2015) One-pot and ultrafast synthesis of nitrogen and phosphorus co-doped carbon dots possessing bright dual wavelength fluorescence emission. Nano 7:17278–17282
24. Zu F, Yan F, Bai Z, Xu J, Wang Y, Huang Y, Zhou X (2017) The quenching of the fluorescence of carbon dots: a review on mechanisms and applications. Microchim Acta 184:1899–1914
25. Rani BK, John SA (2018) Fluorogenic mercury ion sensor based on pyrene-amino mercapto thiadiazole unit. J Hazard Mater 343:98–106
26. Ren XL, Chen ZZ, Chen XY, Liu J, Tang FQ (2014) Sensitive optical detection of alkaline phosphatase activity with quantum dots. J Lumines 145:330–334
27. Jia L, Xu JP, Li D, Pang SP, Fang YA, Song ZG, Ji JA (2010) Fluorescence detection of alkaline phosphatase activity with beta-cyclodextrin-modified quantum dots. Chem Commun 46:7166–7168
28. Liu SG, Li N, Fan YZ, Li NB, Luo HQ (2017) Intrinsically fluorescent polymer nanoparticles for sensing Cu^{2+} in aqueous media and constructing an IMPLICATION logic gate. Sensors Actuators B Chem 243:634–641
29. Xia YS, Zhu CQ (2008) Use of surface-modified CdTe quantum dots as fluorescent probes in sensing mercury (II). Talanta 75: 215–221
30. Zhou L, Lin YH, Huang ZZ, Ren JS, Qu XG (2012) Carbon nanodots as fluorescence probes for rapid, sensitive, and label-free detection of Hg^{2+} and biothiols in complex matrices. Chem Commun 48:1147–1149
31. Lakowicz JR (2006) Principles of fluorescence spectroscopy. Maryland, USA